

Internal Curing of High-Performance Blended Cement Mortars

by Dale P. Bentz

In the twenty-first century, most high-performance concretes, and many other ordinary concretes, are now based on blended cements that contain silica fume, slag, and/or fly ash additions. Because the chemical shrinkage accompanying the pozzolanic and hydraulic reactions of these mineral admixtures is generally much greater than that accompanying conventional portland cement hydration, these blended cements may have an increased demand for additional curing water. When such water cannot be supplied efficiently by external curing, internal curing becomes necessary, if the maintenance of saturated hydration conditions in the blended cement paste is desired. In this paper, the internal curing of three different high-performance blended cement mortars is evaluated with respect to measured autogenous deformation and compressive strength development. Internal curing is particularly beneficial for the mortars containing silica fume or slag blended cements. For the blended cement containing a Type F fly ash, less autogenous deformation is observed, due to the maintenance of a more open (percolated) pore structure containing larger pores, as supported by low temperature calorimetry measurements on hydrated paste specimens. In addition to providing a substantial reduction in autogenous shrinkage at early ages, internal curing also provided a significant increase in long term (28 days and beyond) compressive strength in the three mortars investigated in this study.

Keywords: curing; high performance; mortars.

INTRODUCTION

In the twenty-first century, concretes containing blended cements are becoming the rule rather than the exception. Most cement manufacturers now produce one or more blended cement products, and ready mix producers are generally quite comfortable with blending an ordinary portland cement (OPC) with one or more mineral admixtures during concrete production at their ready mix plants. This is true for both normal-strength and high-performance concretes. It is well known that blended cement concretes may have different curing requirements and exhibit different sensitivity to curing conditions than OPC concretes.¹⁻³

High-performance concrete (HPC) often requires specialized curing procedures to avoid early-age cracking, due at least partially to the earlier depercolation of the capillary pores that occurs in most high-performance mixtures and the self-desiccation and autogenous shrinkage that follow soon thereafter. Also in the twenty-first century, the practice of internal curing (IC) has been developed and demonstrated to substantially reduce autogenous shrinkage and minimize early-age cracking of high-performance mixtures.⁴⁻⁸ In this paper, the IC requirements of three different high-performance blended cement mortars will be examined with respect to autogenous deformation and compressive strength development.

RESEARCH SIGNIFICANCE

The usage of blended cements (whether produced as a blended product by the cement manufacturer or blended at the ready mix plant during concrete production) is becoming

ubiquitous throughout the concrete industry. Blending materials such as silica fumes, slags, and fly ashes participate in pozzolanic reactions with calcium hydroxide produced during conventional portland cement hydration and also may be at least partially hydraulic in their own right (slags for instance). Because these materials each participate in a different set of chemical reactions from those commonly encountered in ordinary portland cement hydration, the accompanying chemical shrinkage is quantitatively different from that of portland cement. For example, while portland cement hydration is typically accompanied by a chemical shrinkage on the order of 0.07 mass of water per mass of cement for complete hydration, for silica fume, slag, and fly ash, these same coefficients are on the order of 0.22, 0.18, and 0.10 to 0.16, respectively. This means that if and when these mineral admixtures react completely in a blended cement system, their demand for curing water (external or internal) can be much greater than that in a conventional ordinary portland cement concrete. When this water is not readily available, due to depercolation of the capillary porosity for example, significant autogenous deformation and (early-age) cracking may result; due to their potentially greater chemical shrinkage, blended cement concretes may also exhibit greater autogenous shrinkage, as has been previously noted for additions of granulated blast-furnace slag.^{9,10} In this study, the influence of IC, supplied via saturated-surface-dry (SSD) lightweight fine aggregates (LWA) on the autogenous deformation and compressive strength development of high-performance blended cement mortars with a bulk water-to-cementitious material ratio (w/cm) of 0.30 is quantified.

EXPERIMENTAL

Materials

Three commercially-available blended cements were obtained from two different cement manufacturers. The characteristics of the cements and their chemical (oxide) compositions as provided by their manufacturers are provided in Table 1. In each case, sufficient samples of the cement were obtained to complete all of the paste and mortar mixtures comprising the present study. The particle size distributions (PSDs) of the three blended cements were measured using a laser diffraction technique. The results presented in Fig. 1 indicate that they have quite similar PSDs, each with a modal diameter near 20 μm (7.9×10^{-4} in.) and a median diameter closer to 10 μm (3.9×10^{-4} in.).

The LWA, an expanded shale, was obtained from an LWA manufacturer. The LWA has an SSD specific gravity of 1.80

ACI Materials Journal, V. 104, No. 4, July-August 2007.

MS No. M-2006-276 received July 6, 2006, and reviewed under Institute publication policies. Copyright © 2007, American Concrete Institute. All rights reserved, including the making of copies unless permission is obtained from the copyright proprietors. Pertinent discussion including authors' closure, if any, will be published in the May-June 2008 ACI Materials Journal if the discussion is received by February 1, 2008.

ACI member Dale P. Bentz is a Chemical Engineer, Building and Fire Research Laboratory, National Institute of Standards and Technology, Gaithersburg, Md. He is a member of ACI Committees 231, Properties of Concrete at Early Ages; 236, Material Science of Concrete; and 308, Curing Concrete.

Table 1—Characteristics and overall compositions of blended cements used in study

Designation	SF	Slag	FA
Blending agent	Silica fume	Slag (GGBFS [*])	Fly ash (Type F [†])
Mass fraction	8%	20%	25%
Blended cement specific gravity (with one standard deviation)	3.10 ± 0.01	3.16 ± 0.01	3.18 ± 0.01
CaO	57.9%	58.8%	Not reported
SiO ₂	25.9%	22.6%	Not reported
Al ₂ O ₃	4.9%	5.8%	Not reported
Fe ₂ O ₃	2.4%	2.4%	Not reported
MgO	3.2%	4.5%	Not reported
SO ₃	2.8%	2.7%	Not reported
Loss on ignition	1.5%	1.5%	Not reported
Free lime	0.6%	Not reported	Not reported
Equivalent alkalis	0.72%	0.6%	Not reported

^{*}GGBFS = ground granulated blast furnace slag.

[†]Type F according to ASTM C 311-05.¹¹

Table 2—Measured particle size distribution of LWAs

Sieve no.	Opening, mm (in.)	Percent passing
4	4.75 (0.187)	98.6
8	2.36 (0.093)	70.1
16	1.18 (0.046)	44.7
30	0.6 (0.024)	29.6
50	0.3 (0.012)	20.4
100	0.15 (0.006)	14.5
Pan	0 (0)	0.0

± 0.05 (one standard deviation) and a measured desorption of 22.6% by mass when the SSD LWA was exposed to a salt solution of potassium nitrate (equilibrium relative humidity [RH] of 93%). The total absorption capacity of the LWA was 23.8% by mass as measured by drying an SSD sample in a desiccator. The size distribution of the LWA was determined by sieving for the purpose of replacing a similar distribution of normalweight sand in the mortar mixtures with IC; the measured size distribution is provided in Table 2. This replacement was performed on a volume basis, so that for each blended cement mortar system, the control and internally cured mixtures will have the same volume of paste.

Low temperature calorimetry

Low temperature calorimetry (LTC) scans were conducted to determine the ages at which depercolation of the capillary porosity occurs for the different blended cements. Small pieces of the hydrated cement pastes ($w/cm = 0.3$, prepared with the same water-reducing admixture dosage as the mortar mixtures described in the following) cured under saturated conditions were used in the LTC experiments. Sample mass was typically between 30 and 90 mg (0.001 and 0.003 oz). For each LTC experiment, one small piece of the relevant cement paste was surface dried and placed in a small open stainless steel pan. The pan with the sample,

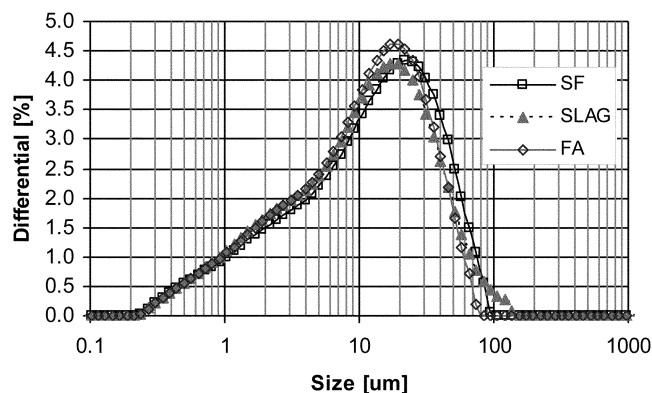


Fig. 1—Measured differential particle size distributions for three blended cements used in study. (Each curve shown is average of six measurements and standard deviations would lie within size of symbols used. One micrometer is equivalent to 3.9×10^{-5} in.)

along with an empty reference pan of similar mass to the empty sample pan, was placed in the calorimeter cell. Using a protocol developed previously,^{12,13} a freezing scan was conducted between 5 and -55 °C (41 and -67 °F) at a scan rate of -0.5 °C/minute (-0.9 °F/minute). The equipment manufacturer has specified a constant calorimetric sensitivity of $\pm 2.5\%$ and a root-mean-square baseline noise of $1.5 \mu\text{W}$, for temperatures between -100 and 500 °C (-148 and 932 °F). The peaks observed in a plot of heat flow (normalized to the mass of the sample) versus temperature correspond to water freezing in pores with various size entryways (pore necks).^{12,13} The smaller the pore entryway, the more the freezing peak is depressed. In the current study, the presence or absence of a peak near -15 °C (5 °F) is used to infer the percolation/depercolation state of the capillary pore network in the hydrating cement pastes.¹³ One advantage of LTC over mercury intrusion porosimetry, and other techniques for assessing pore size and connectivity, is that specimens are evaluated without any applied drying that might damage the pore structure.

Chemical shrinkage

To have an estimate of the IC water demand of the various blended cements, their chemical shrinkages were measured using the ASTM C 1608 standard test method.¹⁴ While the standard recommends a w/cm equals 0.4 paste, in this study, to avoid any chance of bleeding, $w/cm = 0.35$ cement pastes were prepared and evaluated at 25 °C (77 °F). While the mortar mixtures and cement pastes for the low-temperature calorimetry experiments were prepared with a $w/cm = 0.3$, $w/cm = 0.35$ pastes were prepared for the chemical shrinkage measurements to prolong the measurement period (time) before depercolation of the capillary pores occurs at which point the measured water imbibition will fall below the true chemical shrinkage value for the paste. According to the ASTM standard, the expected precision for the test is 0.0042 kg (0.0093 lb) of water per kg (lb) of cement. For these experiments, three replicate specimens of each paste were prepared and the mean value of the chemical shrinkage reported, as shown in Fig. 2.

Mortar mixtures

For each blended cement, two $w/cm = 0.3$ mortar mixtures were prepared. The first, a control mixture with no internal

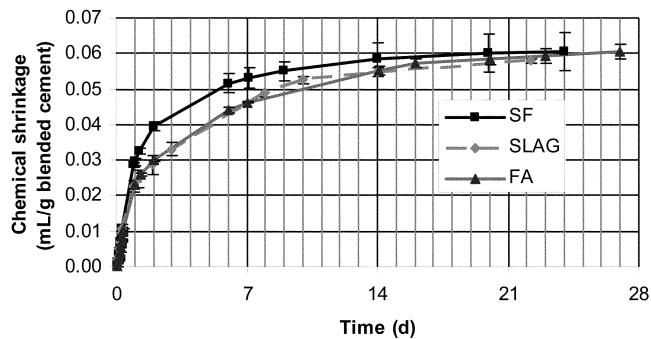


Fig. 2—Measured chemical shrinkage for $w/cm = 0.35$ blended cement pastes cured under saturated conditions at 25 °C (77 °F). 1 mL water/g cement is equivalent to 1 lb water/lb cement. (Error bars indicate \pm one standard deviation for three replicate specimens for each paste and, in some cases, fall within size of plotted symbols.)

curing, and the second, a mixture with an extra 0.08 mass units of IC water per unit mass of blended cement, supplied by the SSD LWA. Other than a change in the specific cement used, the mixture proportions were identical for the three blended cements and are provided for the control and IC mixtures in Table 3. For both mixtures, a blend of four normalweight sands (specific gravity of 2.61) that has been shown to provide improved particle packing for high-performance mortars was employed. As mentioned previously, the size distributions of the four normalweight sands and the LWA were measured so that the LWA could replace an equivalent distribution of normalweight sand in the mixture employing IC. The SSD LWA was prepared by first oven drying the LWA, cooling it to room temperature, and then mixing it in a sealed plastic container with the appropriate mass of water. The prewetted LWA in the sealed container was then placed in an environmental chamber maintained at 25 °C (77 °F) for a minimum of 24 hours.

The mortars were prepared in an epicyclic mixer, with the water and water-reducing admixture being placed in the mixing bowl first. Mixing was performed according to ASTM C 305-99.¹⁶ The unit weight of the fresh mortar was measured and sealed corrugated tubes and 50 mm (2 in.) cubes were prepared for the measurement of autogenous deformation and compressive strength development, respectively. Curing of the mortar specimens was conducted under sealed conditions (double sealed bagging) at 25 °C (77 °F).

Autogenous deformation and compressive strength

Autogenous deformation was assessed using the dilatometer developed by Jensen and Hansen.^{17,18} Corrugated low-density polyethylene tubes were carefully filled with the fresh mortar and sealed with two plastic end caps. The corrugated tubes were supported along their entire length before setting and their length was then periodically assessed using a digital dilatometer. Throughout the 56-day measurement period, the corrugated tube specimens and the dilatometer equipment were kept in a walk-in environmental chamber that was nominally maintained at 25 °C (77 °F). While the temperature of the environmental chamber was not continuously monitored, at the times it was observed, it was always found to be within 0.5 °C (1 °F) of the setpoint. This measurement technique is currently

Table 3—Mortar proportions used in study

Material	Control mixture, g (lb)	IC mixture, g (lb)
Blended cement	2000 (4.405)	2000 (4.405)
Water	584.6 (1.288)	584.6 (1.288)
Water-reducing admixture (assumed 60% water by mass)	25.6 (0.056)	25.6 (0.056)
F95 fine sand*	950 (1.982)	696.1 (1.533)
Graded sand (ASTM C 778 ¹⁵)	722 (1.590)	613.2 (1.351)
20-30 sand (ASTM C 778 ¹⁵)	722 (1.590)	576.9 (1.271)
GS16 coarse sand*	1406 (3.097)	704.9 (1.553)
SSD LWA	—	833.7 (1.836)
Water in SSD LWA	—	160 (0.352)

*F95 and GS16 correspond to sand supplier designations.

under development as an ASTM standard test method within the ASTM C 09.68 Volume Change subcommittee; in the draft standard, the single laboratory precision is listed as 30 microstrains for mortar specimens. In this study, measurements were made on three replicate specimens with the mean value being reported. Mortar cube compressive strengths were measured on three replicate specimens after 3, 8, 28, and 56 days of sealed curing at 25 °C (77 °F), using a mechanical testing machine, at a loading rate of 20.7 MPa/minute (3000 psi/minute), switching to deformation control once a load of 13.8 MPa (2000 psi) was reached.

RESULTS AND DISCUSSION

Low temperature calorimetry—curing water mobility

As indicated in the Experimental section, LTC was used to examine the percolation state of the capillary porosity of the various blended cement pastes as a function of hydration age. Figure 3 presents the results for the three $w/cm = 0.3$ blended cement pastes after 1, 2, or 3 days of saturated curing at 25 °C (77 °F). The presence or absence of a peak at approximately -15 °C (5 °F) indicates a percolated or depercolated capillary pore network, respectively.¹³ The peaks near -25 and -42 °C (-13 and -44 °F) correspond to water freezing in pores that are surrounded (connected) by open gel pores and dense gel pores, respectively.¹³ Once the capillary pores depercolate, it will be much more difficult to provide adequate curing water from an exterior surface (external curing), reinforcing the need for some type of IC. Furthermore, when present, the height of the LTC peak at -15 °C (5 °F) provides a good indication of the volume of percolated capillary pore water remaining in the specimen.¹⁹

For the pastes cured for 1 day, all three blended cement pastes still exhibit a considerable volume of percolated capillary pores. Because a smaller LTC peak indicates less percolated capillary porosity or equivalently more hydration, the heights of the three -15 °C (5 °F) peaks at 1 day would suggest that, in terms of early age reactivity, the system with the silica fume is the most reactive, followed by the one with the slag, and finally by the fly ash blended cement. This order is in agreement with the generally accepted relative reactivities of these three blending components.²⁰⁻²² For an ordinary portland cement paste with $w/cm = 0.3$, depercolation of the capillary porosity (via LTC scans) has been observed to occur between 1 and 3 days of saturated curing.¹² The 2-day LTC scans for the blended cements indicate that for the pastes with silica fume and slag additions, the capillary pores do indeed depercolate between 1 and 2 days of saturated

curing, as indicated by the absence of the $-15\text{ }^{\circ}\text{C}$ ($5\text{ }^{\circ}\text{F}$) peak in the 2-day scans. For the blended cement with fly ash, however, the capillary pores remain somewhat percolated after 2 to 3 days of saturated curing. The fly ash is likely to be only mildly reactive during the first days of hydration²² so that at early ages it is functioning much like a diluent that increases the effective w/c of the paste. The 25% fly ash addition present in the FA blended cement would effectively increase the w/c from 0.3 to 0.4. For an ordinary portland cement paste with $w/c = 0.4$, depercolation has been observed to occur between 3 and 7 days of saturated curing.¹² Thus, further LTC scans were conducted for the FA system over curing times beyond 3 days, and as shown in Fig. 4, depercolation was observed to occur between 5 and 7 days of saturated curing.

The LTC results would suggest that IC will be especially useful in blended cements containing silica fume and/or slag where the capillary porosity has been observed to depercolate after less than 2 days of hydration. Because fly ash is much less reactive at early ages than the silica fume or slag, depercolation in blended cements containing fly ash will occur significantly later than in an equivalent w/cm ordinary cement paste. By considering the fly ash as a diluent, however, the depercolation time of the blended cement paste is basically equal to that of an ordinary portland cement paste of the equivalent effective w/cm . From a practical viewpoint, the later depercolation of the capillary pores in the blended cement pastes containing fly ash means that external curing water (if properly applied) can be used efficiently by the hydrating paste for a longer period of time. The application of IC in such systems still may be an option worth considering to continue the hydration under (internally) saturated conditions after the capillary pores do depercolate (beyond 7 days for instance); this will be reinforced by the compressive strength results to be subsequently presented.

Chemical shrinkage—curing water demand and spatial distribution

Chemical shrinkage measurements¹⁴ were made to directly assess the (IC) water demand of the blended cement mixtures.⁷ The measured results over the course of 21 to 28 days of saturated curing are provided in Fig. 2. At an age of 1 day and beyond, the chemical shrinkage of the SF paste exceeds that of the slag and FA pastes. In comparing the chemical shrinkages of these blended cements, at least two factors must be considered. The first is the inherent chemical shrinkage associated with the chemical reactions that each specific mineral admixture undergoes in the cement. These values can be contrasted with the chemical shrinkage of 0.06 to 0.07 kg (0.132 to 0.154 lb) of water per kg (lb) of cement that is commonly observed for ordinary portland cements.⁷ For example, Jensen²³ had provided a chemical shrinkage coefficient of 0.22 for the pozzolanic reaction between silica fume and the calcium hydroxide produced during cement hydration. Based on experimental measurements and a set of hypothesized reactions for a specific slag, Feng et al.²⁴ had arrived at a coefficient on the order of 0.18 for slag. Finally, based on its typical range of SiO_2 contents and a set of hypothesized reactions,²⁵ for Type F fly ash, a coefficient in the range of 0.10 to 0.16 is projected. Thus, in every case, for complete reaction, the chemical shrinkage coefficient associated with the mineral admixture is much greater than that typically associated with an equivalent mass of ordinary portland cement.

The second factor that must be considered, however, is the achieved reactivity of the mineral admixture. Typically, in a

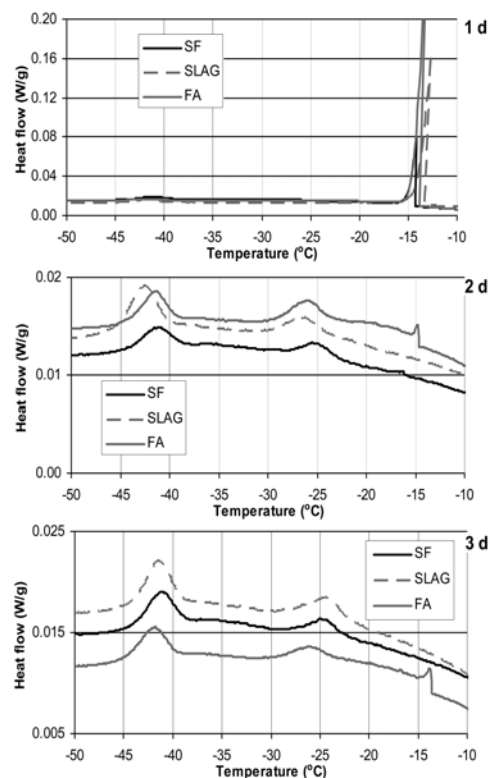


Fig. 3—LTC scans for $w/cm = 0.3$ blended cement pastes after various time periods of saturated hydration at $25\text{ }^{\circ}\text{C}$: 1 day (top), 2 days (middle), and 3 days (bottom). For temperature conversion, $^{\circ}\text{F} = (1.8\text{ }^{\circ}\text{C} + 32)$; for heat flow, $1\text{ W/g} = 1548\text{ BTU}/(\text{h} \cdot \text{lb})$.

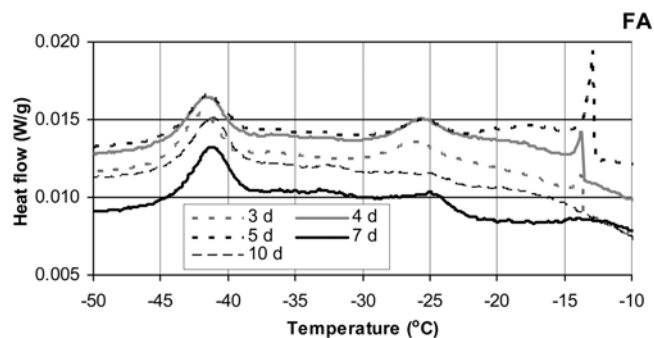


Fig. 4—LTC scans for $w/cm = 0.3$ FA blended cement pastes after various time periods of saturated hydration at $25\text{ }^{\circ}\text{C}$ ($77\text{ }^{\circ}\text{F}$).

blended cement, the achieved degree of hydration of the cement component exceeds that of the mineral admixture.²⁰⁻²² Because the generally accepted reactivity of silica fume is greater than that of slag or fly ash, it is not surprising that this same rank order is maintained in the measured chemical shrinkages presented in Fig. 2. Based on the long term values shown in Fig. 2, and considering that depercolation of the capillary pores is likely occurring in these pastes at ages of 7 days and beyond (perhaps maintaining the measured chemical shrinkage below its true value), it was decided to add 0.08 mass units of water per unit mass of blended cement for each mortar mixture prepared with IC. Of this 0.08 units, based on the measured desorption results for the LWA presented earlier, $0.076 (= 0.08 \times 22.6/23.8)$ units would be expected to be readily available for IC.

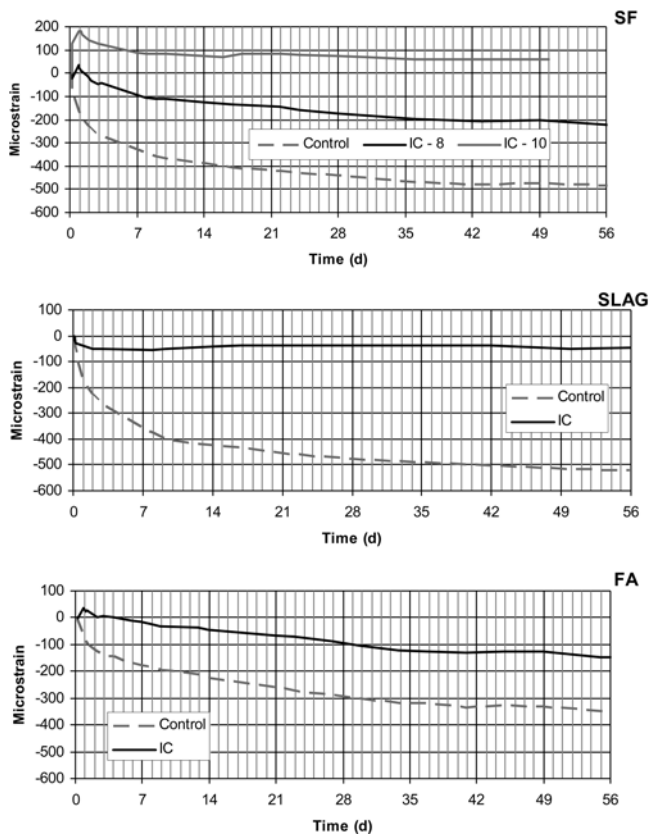


Fig. 5—Autogenous deformation of blended cement mortars: SF (top), slag (middle), and FA (bottom) during 56 days of sealed hydration at 25 °C (77 °F). (For SF system, IC-8, and IC-10 indicate IC additions of 0.08 and 0.10 mass units of water per mass unit of cement, respectively.)

At this level of IC water addition, the spatial distribution of the LWA reservoirs was investigated using a three-dimensional hard core/soft shell microstructural model.^{7,26} Using the mixture proportions from Table 3 and the measured PSDs of the sands, it was determined that 30% of the hydrating cement paste would be within 50 μm (0.002 in.) of an LWA reservoir surface, 63% would be within 100 μm (0.0039 in.), and 96% would be within 200 μm (0.0079 in.). Once the capillary pores depercolate at ages of 2 to 7 days for the mixtures investigated in this study, water transport may become limited to distances of 100 to 200 μm (0.0039 to 0.0079 in.).²⁷ Thus, according to this microstructural simulation, even at later ages, the IC water will be well distributed within the three-dimensional volume and should be readily available for continuing the hydration of the surrounding cement paste.

Autogenous deformation

The measured results for autogenous deformation of the three blended cement mortars with and without IC are provided in Fig. 5. In each case, the application of IC is seen to provide a significant reduction in the observed autogenous deformation during the first 56 days of sealed hydration. For the FA and slag blended cement mortars, the IC is seen to nearly eliminate the autogenous shrinkage (microstrains of less than 100 at 28 days), while for the SF mortar, even with the IC providing approximately 0.08 mass units of extra curing water per unit mass of cement, substantial autogenous shrinkage is observed to occur between 3 and 56 days of

Table 4—Measured mortar cube compressive strengths for various mixtures

Mixture	3-day strength, MPa	8-day strength, MPa	28-day strength, MPa	56-day strength, MPa
SF—control	68.1 (2.0)* 9878 psi	80.4 (3.0) 11,665 psi	—	98.0 (2.7) 14,232 psi
SF—IC (8)	67.9 (4.6) 9843 psi	87.9 (4.6) 12,743 psi	—	105.6 (6.9) 15,312 psi
SF—IC (10)	66.7 (1.4) 9670 psi	85.0 (2.9) 12,327 psi	93.3 (4.7) 13,531 psi	—
Slag—control	60.9 (0.9) 8827 psi	71.5 (2.0) 10,376 psi	81.8 (3.2) 11,863 psi	84.3 (5.7) 12,226 psi
Slag—IC	59.2 (4.2) 8581 psi	71.7 (2.3) 10,399 psi	88.8 (3.9) 12,873 psi	94.6 (1.0) 13,729 psi
FA—control	58.0 (0.5) 8407 psi	70.5 (3.3) 10,224 psi	85.3 (3.4) 12,365 psi	95.3 (4.0) 13,827 psi
FA—IC	57.4 (2.3) 8324 psi	67.5 (3.5) 9794 psi	92.9 (3.8) 13,471 psi	101.1 (2.9) 14,665 psi

*Numbers in parentheses indicate measured standard deviation in MPa for compressive strengths of three replicate cubes at each age for each mixture.

sealed curing. Based on this observation, a separate mortar mixture for the SF cement with 0.10 mass units of extra curing water was prepared and, as shown in the top graph of Fig. 5, this level of IC was sufficient to effectively mitigate the (28-day) autogenous shrinkage of the mortar.

For the control mortars prepared without IC, the measured autogenous deformation for the FA mortar is much less than that for the SF and slag mortars. The shrinkage (deformation) of a partially-saturated porous media under an applied capillary stress can be estimated by^{28,29}

$$\varepsilon = \frac{S\sigma_{cap}}{3} \times \left(\frac{1}{K} - \frac{1}{K_s} \right) \quad (1)$$

where ε is the linear strain or shrinkage, S is the saturation (values between 0 and 1) or fraction of the porosity that is water-filled, σ_{cap} is the stress developed in the pore fluid, K is the bulk modulus of the porous material with empty pores (dry), and K_s is the bulk modulus of the material making up the solid framework of the porous material. In turn, the capillary (tensile) stress in the pore fluid is related to the size of the (assumed cylindrical) pores being emptied by

$$\sigma_{cap} = \frac{(-2\gamma_{lg} \cos \alpha)}{r} \quad (2)$$

where γ_{lg} is the surface tension of the pore solution, α is the contact angle between pore solution and solids (often assumed to be 0 degrees), and r is the radius of the largest (partially) water-filled pore. Based on Eq. (1) and (2), a coarser pore structure should lead to lower capillary stresses and less shrinkage.³⁰ The LTC results presented for the three mortars in Fig. 3 would suggest a more percolated capillary pore structure and higher porosity for the FA control mortar that would be consistent with it having a coarser pore structure and thus less autogenous shrinkage, in agreement with the measured results in Fig. 5. While the SF control mortar likely has a finer pore structure (due to refinement by the very small silica fume particles along with their participation in a pozzolanic reaction with calcium hydroxide), its measured autogenous deformation is slightly less than that of the slag control mortar at ages of 7 days and beyond. As indicated in Eq. (1), this could be due to a higher modulus for the SF

control mortar; compressive strength results supporting this hypothesis will be presented in the following.

Figure 5 shows that the IC basically eliminated further autogenous shrinkage in the slag mortar at ages beyond 1 day. For the internally cured SF (both IC-8 and IC-10) and FA mortars, however, relative to the peak (positive) deformation values observed at 1 day, while long term autogenous shrinkage was substantially reduced when compared with that of the control mortars without IC, it was by no means eliminated. As previously suggested by Jensen and Hansen,¹⁸ in systems containing such pozzolans, a portion of the autogenous shrinkage could be due to decalcification shrinkage, either due to dissolution of calcium hydroxide crystals or reduction in the calcium/silicon ratio of the primary hydration product, namely calcium silicate hydrate (C-S-H) gel.³¹ Powers³² initially suggested this as a mechanism to explain carbonation shrinkage of cement paste.

Compressive strength development

Compressive strengths for the various mortar mixtures are summarized in Table 4, which provides the measured strengths of mortar cubes after 3, 8, 28, and 56 days of sealed curing. For all of the mortars with IC, a strength enhancement on the order of 10% relative to the controls is generally observed at later ages (28 days and beyond) for the mean of the three specimens tested, as increased hydration overcomes any strength reduction due to addition of a porous LWA, in agreement with previous observations on other higher *w/cm* mortars with and without IC that have been subjected to sealed curing.^{6,33} At early ages, the SF mortar provides the highest compressive strengths, followed by the slag mortars and finally the FA mortars, in agreement with the expected relative early age reactivities of the three mineral admixtures and the percolated capillary porosity volume fractions inferred from the 1-day LTC scans presented in Fig. 3. At later ages, the SF mortars maintain the highest strengths, while the FA mortars obtain strengths that exceed those exhibited by the slag ones.

CONCLUSIONS

The incorporation of IC in high-performance blended cement mortars by the addition of saturated LWAs has been shown to be an effective means of drastically reducing autogenous shrinkage. Because autogenous shrinkage is a main contributor to early-age cracking of these materials, it is to be expected that IC would also reduce such cracking. An additional benefit of IC beyond autogenous shrinkage reduction is a significant increase in compressive strength on the order of 10% relative to control specimens at 28 days and beyond (8 days and beyond for silica fume blended cement), under the sealed curing conditions employed in this study. As IC maintains saturated conditions within the hydrating (blended) cement paste, the magnitude of internal self-desiccation stresses are reduced and long-term hydration is increased. IC was found to be particularly effective for the high-performance blended cement mortars containing silica fume and slag, with the silica fume blended cement having the highest demand for (internal) curing water. For the blended cement mortar containing a Type F fly ash, the fly ash appears to function mainly as a diluent at early ages, and the higher and coarser porosity of this mortar resulted in less autogenous shrinkage, even in the control mixture without IC. Thus, properly applied external curing may be effective for a longer period of time in a high-performance fly

ash-cement mortar, with the option of providing IC to continue the maintenance of saturated capillary pores and enhanced hydration (and strength) in the cement paste in the long term.

ACKNOWLEDGMENTS

The author would like to thank M. Peltz and J. Winpiger of the Building and Fire Research Laboratory at NIST for their assistance in preparing the mortar mixtures and measuring the blended cement specific gravities and PSDs. The author would also like to thank Northeast Solite Corporation, Lafarge Canada Inc., and Holcim (US) Inc. for providing materials.

REFERENCES

1. Parrott, L. J., "Influence of Cement Type and Curing on the Drying and Air Permeability of Cover Concrete," *Magazine of Concrete Research*, V. 47, No. 171, 1995, pp. 103-111.
2. Shattaf, N. R.; Alshamsi, A. M.; and Swamy, R. N., "Curing/Environment Effect on Pore Structure of Blended Cement Concrete," *Journal of Materials in Civil Engineering*, V. 13, No. 5, 2001, pp. 380-388.
3. Bentz, D. P., "Influence of Curing Conditions on Water Loss and Hydration in Cement Pastes with and without Fly Ash Substitution," NISTIR 6886, U.S. Department of Commerce, July 2002, 15 pp.
4. Weber, S., and Reinhardt, H. W., "A New Generation of High Performance Concrete: Concrete with Autogenous Curing," *Advanced Cement-Based Materials*, V. 6, 1997, pp. 59-68.
5. Jensen, O. M., and Hansen, P. F., "Water-Entrained Cement-Based Materials: I—Principles and Theoretical Background," *Cement and Concrete Research*, V. 31, No. 4, 2001, pp. 647-654.
6. Geiker, M. R.; Bentz, D. P.; and Jensen, O. M., "Mitigating Autogenous Shrinkage by Internal Curing," *High Performance Structural Lightweight Concrete*, SP-218, J. P. Ries and T. A. Holm, eds., American Concrete Institute, Farmington Hills, Mich., 2004, pp. 143-154.
7. Bentz, D. P.; Lura, P.; and Roberts, J. W., "Mixture Proportioning for Internal Curing," *Concrete International*, V. 27, No. 2, 2005, pp. 35-40.
8. Cusson, D., and Hoogeven, T., "Internally-Cured High-Performance Concrete under Restrained Shrinkage and Creep," *CONCREP 7 Workshop on Creep, Shrinkage, and Durability of Concrete and Concrete Structures*, Nantes, France, Sept. 12-14, 2005, pp. 579-584.
9. Lee, K. M.; Lee, H. K.; Lee, S. H.; and Kim, G. Y., "Autogenous Shrinkage of Concrete Containing Granulated Blast-Furnace Slag," *Cement and Concrete Research*, V. 36, No. 7, 2006, pp. 1279-1285.
10. Lura, P., "Autogenous Deformation and Internal Curing of Concrete," PhD thesis, Technical University Delft, Delft, The Netherlands, 2003, 180 pp.
11. ASTM C 311-05, "Standard Test Methods for Sampling and Testing Fly Ash or Natural Pozzolans for Use in Portland-Cement Concrete," ASTM International, West Conshohocken, Pa., 2005, 9 pp.
12. Snyder, K. A., and Bentz, D. P., "Suspended Hydration and Loss of Freezable Water in Cement Pastes Exposed to 90% Relative Humidity," *Cement and Concrete Research*, V. 34, No. 11, 2004, pp. 2045-2056.
13. Bentz, D. P., and Stutzman, P. E., "Curing, Hydration, and Microstructure of Cement Paste," *ACI Materials Journal*, V. 103, No. 5, Sept.-Oct. 2006, pp. 348-356.
14. ASTM C 1608-05, "Test Method for the Chemical Shrinkage of Hydraulic Cement Paste," ASTM International, West Conshohocken, Pa., 2005, 4 pp.
15. ASTM C 778-05, "Standard Specification for Standard Sand," ASTM International, West Conshohocken, Pa., 2005, 3 pp.
16. ASTM C 305-99, "Standard Practice for Mechanical Mixing of Hydraulic Cement Pastes and Mortars of Plastic Consistency," ASTM International, West Conshohocken, Pa., 1999, 3 pp.
17. Jensen, O. M., and Hansen, P. F., "A Dilatometer for Measuring Autogenous Deformation in Hardening Portland Cement Paste," *Materials and Structures*, V. 28, 1995, pp. 406-409.
18. Jensen, O. M., and Hansen, P. F., "Autogenous Deformation and Change of Relative Humidity in Silica Fume Modified Cement Paste," *ACI Materials Journal*, V. 93, No. 6, Nov.-Dec. 1996, pp. 539-543.
19. Bentz, D. P., "Capillary Porosity Depreciation/Repercolation in Hydrating Cement Pastes Via Low Temperature Calorimetry Measurements and CEMHYD3D Modeling," *Journal of the American Ceramic Society*, V. 89, No. 8, 2006, pp. 2606-2611.
20. Sun, G. K., and Young, J. F., "Quantitative Determination of Residual Silica Fume in DSP Cement Pastes by ²⁹-Si NMR," *Cement and Concrete Research*, V. 23, No. 2, 1993, pp. 480-483.
21. Bentz, D. P.; Waller, V.; and de Larrard, F., "Prediction of Adiabatic Temperature Rise in Conventional and High-Performance Concretes Using a 3-D Microstructural Model," *Cement and Concrete Research*, V. 28, No. 2, 1998, pp. 285-297.

22. Feng, X. P.; Garboczi, E. J.; Bentz, D. P.; Stutzman, P. E.; and Mason, T. O., "Estimation of the Degree of Hydration of Blended Cement Pastes by a Scanning Electron Microscope Point-Counting Procedure," *Cement and Concrete Research*, V. 34, No. 10, 2004, pp. 1787-1793.
23. Jensen, O. M., "Autogenous Deformation and RH-Change—Self-Desiccation and Self-Desiccation Shrinkage," PhD thesis, TR284/93, Building Materials Laboratory, Technical University of Denmark, Lyngby, Denmark, 1993, 117 pp. (in Danish)
24. Feng, X.; Bentz, D. P.; and Stutzman, P. E., "Experimental Studies of Portland Cement/Slag Hydration," Presentation at the 102nd Annual Meeting of the American Ceramic Society, St. Louis, Mo., 2000.
25. Bentz, D. P., and Remond, S., "Incorporation of Fly Ash into a 3-D Cement Hydration Microstructure Model," NISTIR 6050, U.S. Department of Commerce, Aug. 1997, 48 pp.
26. Bentz, D. P.; Garboczi, E. J.; and Snyder, K. A., "A Hard Core/Soft Shell Microstructural Model for Studying Percolation and Transport in Three-Dimensional Composite Media," NISTIR 6265, U.S. Department of Commerce, 1999, 51 pp.
27. Bentz, D. P., and Snyder, K. A., "Protected Paste Volume in Concrete: Extension to Internal Curing Using Saturated Lightweight Fine Aggregates," *Cement and Concrete Research*, V. 29, No. 11, 1999, pp. 1863-1867.
28. Bentz, D. P.; Garboczi, E. J.; and Quenard, D. A., "Modelling Drying Shrinkage in Reconstructed Porous Materials: Application to Porous Vycor Glass," *Modelling and Simulation in Materials Science and Engineering*, V. 6, 1998, pp. 211-236.
29. MacKenzie, J. K., "The Elastic Constants of a Solid Containing Spherical Holes," *Proceedings of the Physics Society*, No. 683, 1950, pp. 2-11.
30. Bentz, D. P.; Jensen, O. M.; Hansen, K. K.; Oleson, J. F.; Stang, H.; and Haecker, C. J., "Influence of Cement Particle Size Distribution on Early Age Autogenous Strains and Stresses in Cement-Based Materials," *Journal of the American Ceramic Society*, V. 84, No. 1, 2001, pp. 129-135.
31. Chen, J. J.; Thomas, J. J.; and Jennings, H. M., "Decalcification Shrinkage of Cement Paste," *Cement and Concrete Research*, V. 36, No. 5, 2006, pp. 801-809.
32. Powers, T. C., "A Hypothesis on Carbonation Shrinkage," *Journal of PCA Research and Development Labs*, V. 4, No. 2, 1962, pp. 40-50.
33. Bentz, D. P.; Halleck, P. M.; Grader, A. S.; and Roberts, J. W., "Direct Observation of Water Movement during Internal Curing Using X-Ray Microtomography," *Concrete International*, V. 28, No. 10, 2006, pp. 39-45.